Manufacturing and Temperature Measurements of a Sodium Heat Pipe

Byoung In Lee
Graduate School, Pusan National University, Pusan 609-735, Korea
Sung Hong Lee*
Research Institute of Mechanical Technology, Pusan National University, Pusan 609-735, Korea

A high-temperature sodium stainless steel heat pipe was fabricated and its performance has been investigated. The working fluid was sodium and it was sealed inside a straight tube container made of stainless steel. The amount of sodium occupied approximately 20% of the total volume of the heat pipe and its weight was 65.7gram. The length of a stainless steel container is 1002mm and its outside diameter is 25.4mm. Performance tests were carried out in a room air condition under a free convective environment and the measured temperatures are presented. The start-up behavior of the heat pipe from a frozen state was investigated for various heat input values between 600W and 1205W. In steady state, axial temperature distributions of a heat pipe were measured and its heat transfer rates were estimated in the range of vapor temperature from 500℃ to 630℃. It is found that there are small temperature differences in the vapor core along the axial direction of a sodium heat pipe for the high operating temperatures. But for the range of low operating temperatures there are large temperature drops along the vapor core region of a sodium heat pipe, because a small vapor pressure drop makes a large temperature drop. The transition temperature was reached more rapidly in the cases of high heat input rate for the sodium heat pipe.

Key Words: Frozen Start-up Limit, Transition Temperature, Heat Transport Limitation, High Temperature Heat Pipe, Liquid Metal, Sodium

Nomenclature

A : Heat transfer surface area[m^2]
C_p : Specific heat[J/kg · ℃]
D : Diameter[m]
g : Gravitational acceleration[m/s^2]
h : Heat transfer coefficient[$W/m^2 \cdot ℃$]
h_{fg} : Latent heat of vaporization[J/kg]
K : Permeability[m^2]
K_n : Knudsen number(λ/D)
k : Thermal conductivity[W/m · ℃]
M : Molecular weight[kg/kmol]
P, p : Pressure[N/m^2]
P_r : Reduced pressure(P/P_c)
Q, q : Heat transfer rate[W]
q'' : Heat flux[W/m^2]
R : Gas constant[J/kg · K]
r : Radius[m]
s : Injection/suction factor
T : Temperature[℃]
T^* : Transition temperature[℃]

Greek Symbols

γ : Specific heat ratio
δ : Liquid film thickness[m]
λ : Mean free path[m]
μ : Viscosity[$N \cdot s/m^2$]
ν : Dynamic viscosity[m^2/s]
ρ : Density[kg/m^3]
σ : Surface tension, condensing coefficient [N/m]

* Corresponding Author,
E-mail : Sunghonglee@yahoo.com
TEL : +82-51-510-2312; **FAX** : +82-51-514-7640
School of Mechanical Engineering, Pusan National University, Pusan 609-735, Korea. (Manuscript **Received** November 17, 2000; **Revised** August 20, 2001)

φ : Porosity of screen wick

Superscript

$-$: Average, universal

Subscripts

a : Atmospheric
b : Boiling
c : Capillary, condenser, critical
e : Evaporator
h : Hydraulic
i : Inner
$inter$: Interphase between vapor and liquids
l : Liquid phase
max : Maximum
n : Critical nucleation
s : Surface/ sonic
si : Inside surface
o : Outer
u : Universal
v : Vapor phase, vapor section
w : Wick, wall

1. Introduction

Heat pipe is an excellent heat transfer device which is able to transfer heat energy without additional power. Since a heat pipe transports heat energy through the phase change phenomena of working fluids with a small temperature difference during its normal operation, this is an effective device for transferring large amounts of heat energy.

Generally, a working fluid is charged in a heat pipe device, for examples, liquid state of water, acetone, etc. for a heat pipe working in low temperature ranges, while a high temperature heat pipe (HTHP) uses a liquid metal as a working fluid. There may be several differences between the two kinds of heat pipes, high and low temperature ranges. The fundamental working principle of a heat pipe is the same. But the design and manufacturing criteria and start-up profiles are different, because the initial phase in a room temperature and the chemicals of the substance used inside heat pipe of the two kinds have significant differences with each other.

The start-up temperature profiles along the axial direction of vapor core of a heat pipe working in low temperature ranges is nearly uniform throughout the start-up period. But in the starting period of high temperature sodium heat pipe frozen initially at the room temperature, vapor temperature of the heat pipe may rise to some intermediate level in heating section and remaine in almost constant value as the steep temperature front moves along the length of the pipe. When the uniform hot zone is expanded to the condenser end zone of the heat pipe from heating zone, the temperature distribution gradually increases to a steady-state level depending on the capacity of input power rates, which is similar to a low temperature heat pipe behavior.

Faghri et al.(1991) fabricated a high temperature sodium-stainless steel heat pipe with multiple heat sources and sinks. They analyzed its performance of the manufactured heat pipe. Jang et al. (1990) and Cao and Faghri (1993) demonstrated that the vapor inside the heat pipe should be the state of continuum flow for normal operation. This condition is satisfied when the surface temperature of evaporator section is greater than a transition temperature (T^*).

$$T^*=\frac{\pi}{2\times10^{-4}}\frac{M}{R_u}\left(\frac{\mu_v}{\rho_v D}\right)^2 \quad (1)$$

Jang (1996) has investigated a performance test of a potassium heat pipe and showed that the heat pipe starts to reach the normal working state when the surface temperature of evaporator section is above the calculated transition temperature of 567K. Ko and Lee (2000) reported the transient temperature of 683K for a sodium heat pipe. In the present investigation, the transition temperature was 693K.

Several researchers studied axial temperature distribution of heat pipes in a steady state. Cotter (1965) made the earliest theoretical treatment of the heat pipe. Faghri(1995) made generalized equations for approximate analytical solutions by using axial average vapor velocity of the working fluid and heat input rates.

In this investigation, a sodium heat pipe which is operating between 500℃ and 1000℃ has been made and its performance tests were carried out in

a room air under free convection conditions around the condenser zone of the heat pipe. The start-up behavior of the heat pipe from a frozen state, axial temperature distributions in a steady state, boiling heat transfer coefficients and condensation heat transfer coefficients were investigated by measuring vapor and surface temperatures of a sodium heat pipe.

2. Experimental Apparatus and Procedure

2.1 Sodium heat pipe

A straight circular tube type heat pipe containing metallic sodium which is usually used in a high temperature heat pipe has been produced. The compatibility of the tube material(316L stainless steel) with sodium is well-documented in heat pipe literatures. A simple circumferential screen wick, which consist of two wraps of 60 mesh 316 stainless steel, was installed to provide liquid return path to the evaporator section. The amount of sodium occupied is approximately 20% of the total inner volume of the heat pipe and its weight is 65. 7 gram. Figure 1 shows sketched details of the heat pipe and Table. 1 shows specifications of the heat pipe.

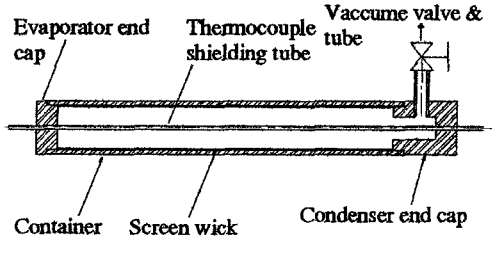

Fig. 1 Sketched details of a heat pipe

Table 1 Specification of a heat pipe

Working fluid	Sodium 65.7 gram
Container	Seamless Stainless Steel 316L, ϕ25.4 1.65t, 990mm length
Bottom Cap	Stainless Rod 316L, 10mm length
Top Cap	Stainless Rod 316L, 30mm length
Wick	Stainless Steel 316, 60mesh×2 Layers
Thermocouple shielding tube	Seamless Stainless Steel 316L, ϕ5.0 1.0t, 1040mm length

The length of heating zone of the heat pipe is 0.425m, that of adiabatic zone is 0.15m, and that of condensor region in the air is 0.425m. The maximum heat transport capacity depends strongly on the working fluid and its temperature. The maximum axial heat transfer rate of a particular heat pipe under certain working conditions can be determined by a number of possible heat transfer limitations. The limitations will depend on the geometry of the heat pipe, the wick structure, the vapor channel shape, the working fluid and the operating temperature. Maximum heat transport limitations may be calculated by Eqs. (2)-(5), which are summarized by Chi (1976). Figure 2 shows that entrainment limitation is one of the most important factor in the present investigation of sodium heat pipe.

Capillary limitation

$$Q_{c,\max}=\frac{2\left(\frac{\sigma\rho_l h_{lv}}{\mu_l}\right)\left(\frac{K}{r_c}\right)(2\pi r_v t_w)}{0.5L_e+L_a+0.5L_c} \tag{2}$$

Sonic limitation

$$Q_{s,\max}=A_v\rho_v h_{lv}\left[\frac{\gamma_v T_v r_v}{2(\gamma_v+1)}\right]^{1/2} \tag{3}$$

Entrainment limitation

$$Q_{e,\max}=A_v h_{lv}\left(\frac{\sigma\rho_v}{2r_{h,s}}\right)^{1/2} \tag{4}$$

Boiling limitation

$$Q_{b,\max}=\frac{2\pi L_e k_e T_v}{h_{lv}\rho_v \ln(r_i/r_v)}\left(\frac{2\sigma}{r_n}-P_c\right) \tag{5}$$

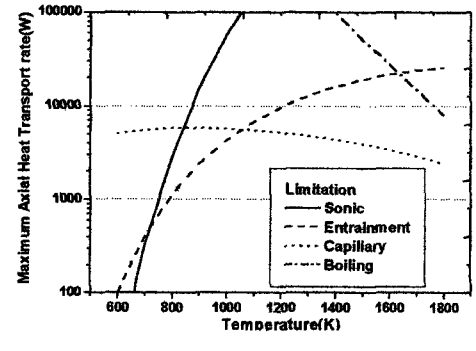

Fig. 2 Heat transport limitation of a testing heat pipe

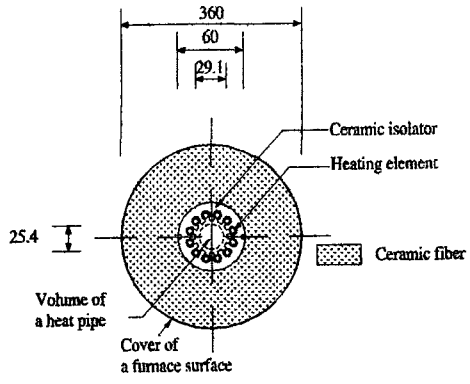

Fig. 3 Section view of the test furnace (unit: mm)

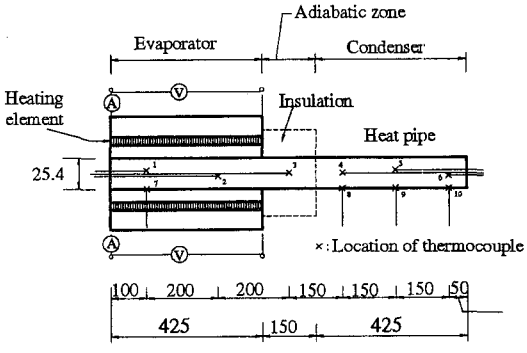

Fig. 4 Locations of thermocouple(unit : mm)

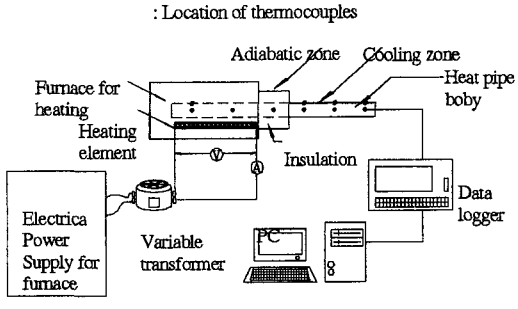

Fig. 5 Schematic diagram of the experimental equipment

3. Measurement of Temperature and Performance Test

3.1 Heating furnace

To supply heat energy to the heating (evaporator) section of a heat pipe, a heating furnace was constructed. Figure 3 illustrates details of the furnace heater. The heating elements of an electrical resistance are located in a ceramic insulator in the core. Power supply can be controlled by a variable electrical transformer attached to the furnace. Most of space between the ceramic core region and the surface cover is filled with ceramic fiber which is used to protect heat loss. A digital multimeter was used to measure electrical power supply to the heater.

3.2 Temperature measurement of surface and vapor core of a sodium heat pipe

To measure the surface temperature of heat pipe, one thermocouple in evaporating region and three thermocouples in condensing region (K-type) were installed on the surface of the heat pipe wall by spot welding and silver soldering. A small thermocouple shielding tube was axially inserted into the heat pipe center line. Six thermocouples (K-type) are arranged inside the small tube to measure the axial vapor temperatures of the heat pipe core region and those thermocouples are connected with thermometer through the evaporator end cap and condenser end cap of the testing heat pipe. Temperatures measured directly by the thermocouple are considered as the inner vapor temperatures of the heat pipe. This is an acceptable assumption because there is no heat input and heat output through the thermocouple shielding tube. All thermocouples were connected to a data logger and the data were stored on a personal computer. Locations of thermocouples which measure surface and vapor temperatures of the heat pipe are shown in Fig. 4. The total performance testing system is shown in Fig. 5.

3.3 Experimental procedure

Performance tests are carried out for two purposes. The one is to understand the behavior of the frozen start-up in unsteady state process and the other is to investigate axial temperature distributions and boiling and condensation heat transfer coefficients in steady state under the radiation and free convection heat transfer condition in a room air in the cooling section of sodium heat pipe.

For the unsteady state tests, vapor temperatures and other measurements were recorded at every 5 minutes interval during 300 minutes after heat inputs began. After 300 minutes elapsed from the beginning of a test, the change of temperature is negligible. Therefore, 300 minutes are regarded as the required time for steady state in the present investigation. For the steady state tests, the voltage and the current supplied to the evaporator, vapor and surface temperatures are recorded through a data acquisition system after a steady state was reached.

4. Experimental Results and Discussion

4.1 Frozen start-up behavior

The axial vapor temperature distribution along the heat pipe shows the behavior of the frozen start-up in Fig. 6. The vapor temperatures at the evaporator zone is increased rapidly up to the transition temperature, while then vapor temperatures at the condenser zone remains at the initial temperature. Then, large axial temperature gradients are developed between the evaporator and condenser sections even though then vapor temperatures at the evaporator are higher than the melting temperature of sodium.

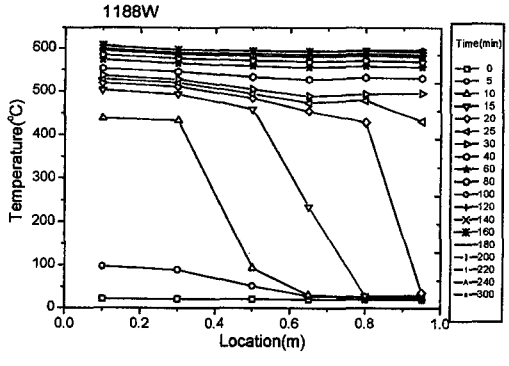

(a) Input power = 1188W

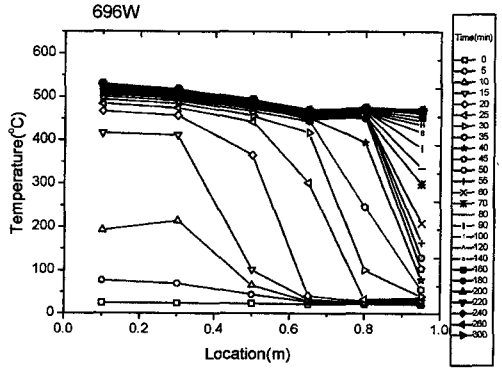

(b) Input power = 696w

Fig. 6 Transient axial vapor temperature profiles along a heat pipe during a frozen startup period

When temperatures at the evaporator rise above the transition temperature, the increasing rate of temperature at the evaporator is slowed down and the temperature of evaporator zone becomes near isothermal. The temperature increase at the adjacent condenser region is accelerated. While temperatures at the condenser zone is increased to the transition temperature, those at the evaporator are remained almost constant until the end of condenser exceeded the transition temperature. These kinds of temperature profiles imply that the vaporization of the working fluid at the evaporator and the vapor flow in the vapor space are significant during this start-up period. When the axial vapor temperature profiles becomes nearly uniform, the axial heat pipe temperatures of sodium vapor may be increased further until steady state conditions are established, similar to a low temperature range heat pipe.

In this investigation, it takes 25 minutes to reach the transition temperature in case of heat input power 1188W, but 35 minutes in case of 1157W, 40 minutes in 848W, 50 minutes in 848W and 100 minutes in power level of 696W. This means that larger heat inputs yield faster startups and continuous vapor flows because evaporation can take place more rapidly at the liquid-vapor interface and the vapor density is increased more rapidly as heat power input is increased. Figure 6 shows that vapor temperature at position 0. 95m from the end of evaporator side of heat pipe is changing more slowly than temperatures at any other locations because most of power input is used for increasing the vapor density and the rest is transfered from condenser region to surroundings.

4.2 Axial vapor temperature distribution in steady state

Axial measured vapor temperature profile along a heat pipe in steady state is compared with prediction calculated by Cotter's (1965) and Fighri's correlations (1995). Figure 7 shows that temperature values predicted by Cotter's correlation are higher than those by Faghri's. The predicted temperature values are decreased along a vapor moving direction from evaporation to adiabatic region, but increased in condenser region. In Figure 7(a), the experimental data are located in the intermediate zone between two predicted correlations in evaporation and adiabatic region. But those are located below the two predition values by Faghri's and Cotter's correlations in condenser region. Figure 7(b) shows that measured temperature drops along a sodium heat pipe are larger than the two predictions of Faghri and Cotter. However, magnitude of temperature drops in Fig. 7 (a) is much larger than that in Fig. 7(b). Steady state temperature profiles of vapor core region are presented in Fig. 8. It is observed that the magnitude of maximum temperature difference of axial temperature distribution is reduced along the sodium heat pipe when heat input power level is increased.

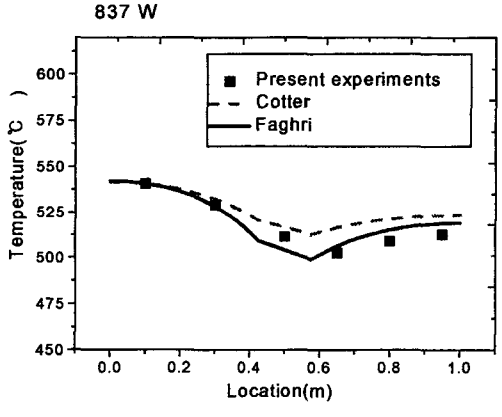

(a) Input power = 837 W

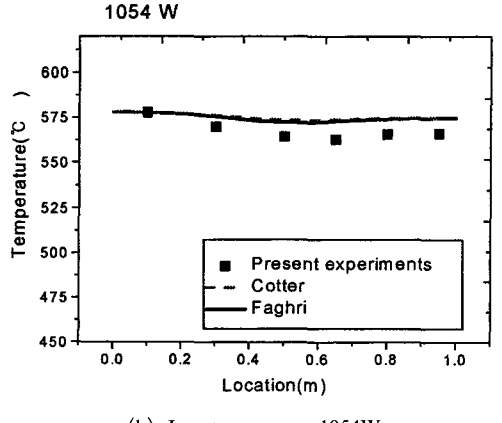

(b) Input power = 1054W

Fig. 7 Comparison of measured vapor temperature distribution with Faghri's and Cotter's correlation

4.3 Boiling heat transfer coefficients

Heat transfer inside evaporator region of a heat pipe may be analyzed by nucleate pool boiling. Both of vapor temperature and outer surface temperature are measured at the location of 0.10m from the end of evaporator side of a heat pipe in steady state. Inside evaporator surface temperature(T_{si}) at the location of 0.10m may be calculated in each case of heat inputs by using Fourier's law. Then, boiling heat transfer coefficients can be estimated by following Eq.

$$h_b = \frac{Q_e}{A_e(T_{si} - T_v)} \tag{6}$$

In Fig. 9, the boiling heat transfer coefficients obtained from present experiments are compared with the calculation by Subbotin's and Kutateladze's correlation, which are nucleate pool boiling correlations. Figure 9 shows that boiling heat transfer coefficients agree well with Subbotin's correlation within 30 percent error.

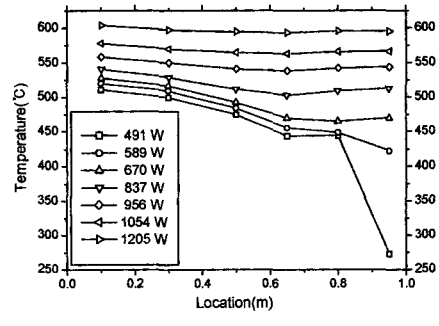

Fig. 8 Steady state axial temperature profiles of vapor core in a sodium a heat pipe depending on input power level

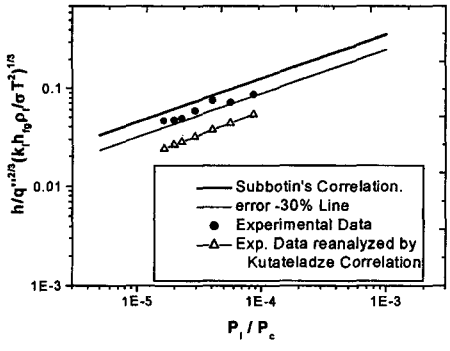

(a)

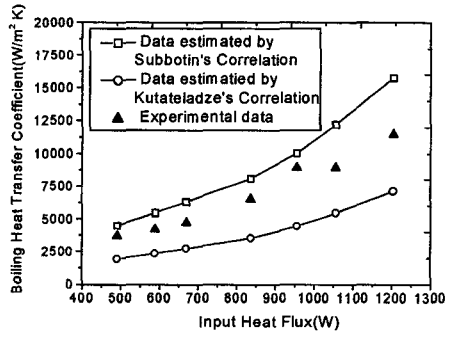

(b)

Fig. 9 Comparison of boiling heat transfer coefficients with predicted values

Subbotin's Correlation(Carey, 1992):

$$h_b=C_s(q'')^{2/3}\left(\frac{k_l h_{lv}\rho_l}{\sigma T^2}\right)^{1/3}\left(\frac{P_l}{P_c}\right)^s \qquad (7)$$

$$C_s=8.0,\ S=0.45 \text{ for } \frac{P_l}{P_c}<0.001$$

$$C_s=1.0,\ S=0.15 \text{ for } \frac{P_l}{P_c}\geq 0.001$$

Kutateladze's Correlation(1952):

$$h_b=7.0\times10^{-4}\times\frac{k_l}{l_l}\times\left(\frac{q''l_l}{h_{lv}\rho_v\nu_l}\right)^{0.7}\times P_r^{0.35}\times\left(\frac{Pl_l}{\sigma}\right)^{0.7} \qquad (8)$$

$$l_l=\sqrt{\frac{\sigma}{g(\rho_l-\rho_v)}}$$

4.4 Condensation heat transfer coeffients

In this investigation, vapor temperatures and surface temperatures were obtained at locations of 0.65, 0.80, 0.95m from the end of evaporator side of heat pipe in the steady state to calculate condensation heat transfer coefficients. Average condensation heat transfer coefficients($\bar{h}_c$) may be

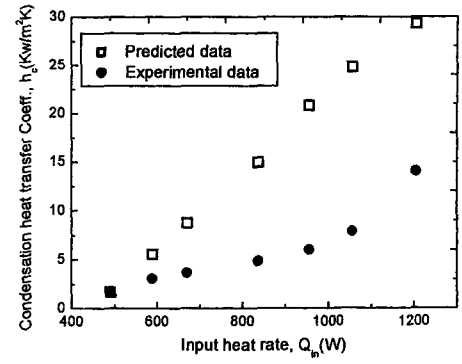

Fig. 10 Experimental data of condensation heat tran sfer coefficients

estimated based on experimental data(Lee et al.) by Eq. (9).

$$\bar{h}_c=\frac{Q_c}{A(\bar{T}_v-\bar{T}_{si})} \qquad (9)$$

It is also expected there exist large liquid-vapor interfacial temperature drops at low pressure in condensate film of liquid metal near wick zone. Magnitude of liquid-vapor interfacial temperature drops may be calculated by using Eq. (10) which is proposed by Silver and Simpson (1961) and Sukhatme and Rohsenow (1996) proposed condensation coefficient $\sigma=0.45$ in liquid metal. Temperature drops in condensate film (wick zone) may be calculated by Nusselt's analysis, because heat transfer in condensate film may be considered as conduction due to the high conductivity of liquid metal. Average inside surface temperature of condenser($\bar{T}_{si}$) can be obtained from known temperatures in this predicted method.

$$\frac{Q}{A}=\left(\frac{\sigma}{2-\sigma}\right)\left(\frac{2}{\pi}\right)^{0.5}\left(\frac{M}{R_u}\right)^{1.5}\frac{p_v h_{lv}^2}{T_v^{2.5}}(T_v-T_{inter}) \qquad (10)$$

5. Conclusion

A high-temperature stainless steel heat pipe with sodium as a working fluid was fabricated and its performance has been investigated.

(1) As heat input rate increase, it takes a shorter time to reach a uniformly distributed axial temperature profile of steady state along a sodium heat pipe from a frozen start-up period.

(2) In steady state, axial vapor temperature profile of a sodium heat pipe agrees well with Cotter's and Faghri's correlation. The higher operating temperature of a sodium heat pipe increases, the smaller temperature difference along an axial vapor temperature distribution becomes.

(3) Boiling heat transfer coefficients become large as the heat input rate increases and they agree well with Subbotin's correlation (within 30 %).

Reference

Carey, V. P., 1992, *Liquid-vapor Phase Change Phenomena*, Hemisphere Pub. Corp.

Cao, Y. and Faghri, A., 1993, "A Numerical Analysis of High-Temperature Heat Pipe Startup From the Frozen State," *Journal of Heat Transfer*, Vol. 115, pp. 247~254.

Chi, S. W., 1976, *Heat Pipe Theory and Practice : A Source Book*, 2nd ed., Hemisphere Pub. Corp.

Collier, J. G. and Thome, J. R., 1996, *Convective Boiling and Condensation*, 3rd ed., Clarendon Press, Oxford, Chapter 10, pp. 436~438.

Cotter, T. P., 1965, "Theory of Heat Pipes," Los Alamos Scientific Laboratory Report No. LA-3246-MS.

Faghri, A. Buchko, M and Cao, Y., 1991, "A Study of High Temperature Heat Pipes With Multiple Heat Sources and Sinks," *Journal of Heat Transfer*, Vol. 113, pp. 1003~1009.

Faghri, A., 1995, *Heat Pipe Science and Tech nology*, Taylor & Francis.

Jang, J. H. Faghri, A. Chang, W. S. and Mahefkey, E. T., 1990, "Mathematical Modeling and Analysis of Heat Pipe Start-Up From the Frozen State," *Journal of Heat Transfer*, Vol. 112, pp. 586~594.

Jang, J. H., 1996, "Performance Characteristics of Liquid Metal Heat Pipes - A Potassium Heat Pipe," *Proc. of the 3rd KSME-JSME Thermal Engineering Conference*, Vol. I, pp. 89~94.

Ko, Y. K. and Lee, S. H., 2000, "Manufacturing and Performance Test of a High-temperature Sodium Heat Pipe," *Proc. 5th International Symposium on Heat Transfer*, pp. 680~685, Beijing.

Kutateladze, S. S., 1952, "Heat Transfer in Condensation and Boiling," 2nd ed., *Mashgiz*, Moscow, *AEC Translation 3770*, U.S. AEC Tech. Info. Service.

Lee, S. H., Ko, Y. K., Lee, B. I. and Lee, Y., 2000, "Manufacturing and Operation Test of a High Temperature Sodium Heat pipe," *Proc. 4th JSME-KSME Thermal Engineering conference*, Vol. 1, pp. 567~572, Kobe.

Silver, R. S. and Simpson, H. C., 1961, "The Condensation of Superheated Steam," *Proc. Nat. Engng. Lab. Conf.*, Glasgow, Scotland.

Sukhatme, S. P. and Rohsenow, W. M., 1996, "Heat Transfer During Film Condensation of a Liquid Metal Vapor," *ASME J. of Heat Transfer*, pp. 19~28.